Shining light on transition metal oxides: unveiling the hidden Fermi Liquid

Xiaoyu Deng,[1] Aaron Sternbach,[2] Kristjan Haule,[1] D. N. Basov,[2] and Gabriel Kotliar[1]

[1] *Department of Physics and Astronomy, Rutgers University, Piscataway, New Jersey 08854, USA*
[2] *Department of Physics, University of California-San Diego, La Jolla, California 92093, USA*

(Dated: April 28, 2014)

We use low energy optical spectroscopy and first principles LDA+DMFT calculations to test the hypothesis that the anomalous transport properties of strongly correlated metals originate in the strong temperature dependence of their underlying resilient quasiparticles. We express the resistivity in terms of an effective plasma frequency ω_p^* and an effective scattering rate $1/\tau_{tr}^*$. We show that in the archetypal correlated material V_2O_3, ω_p^* increases with increasing temperature, while the plasma frequency from partial sum rule exhibits the opposite trend . $1/\tau_{tr}^*$ has a more pronounced temperature dependence than the scattering rate obtained from the extended Drude analysis. The theoretical calculations of these quantities are in quantitative agreement with experiment. We conjecture that these are robust properties of all strongly correlated metals, and test it by carrying out a similar analysis on thin film $NdNiO_3$ on $LaAlO_3$ substrate.

PACS numbers: 71.27.+a, 72.10.-d, 78.20.-e

arXiv:1404.6480v1 [cond-mat.str-el] 25 Apr 2014

Understanding the transport properties in metallic states of strongly correlated materials is a long-standing challenge in condensed matter physics. Many correlated metals are not canonical Landau Fermi liquids (LFL) as their resistivities do not follow the T^2 law in a broad temperature range. Fermi liquid behavior emerges only below a very low temperature scale, T_{LFL}, which can be vanishingly small or hidden by the onset of some form of long range order. Above T_{LFL}, the resistivity usually rises smoothly and eventually exceeds the Mott-Ioffe-Regel limit, entering the so-called "bad metal" regime[1] with no clear sign of saturation [2, 3]. As stressed in Ref. 1 an interpretation of the transport properties in terms of quasiparticles (QPs) is problematic when the mean free path is comparable with the de Broglie wavelength of the carriers and describing the charge transport above T_{LFL} is an important challenge for the theory of strongly correlated materials.

It was shown in the context of the interacting electron phonon system, that the QP picture is actually valid in regimes that fall outside the LFL hypothesis[4]. There are peaks in the spectral functions which define renormalized QPs even though the QP scattering rate is comparable to the QP energy. The transport properties can be formulated in terms of a transport Boltzman kinetic equation for the QP distribution function, which has precisely the form proposed by Landau. Solving the transport equation, the dc conductivity can be expressed as

$$\sigma_{dc} = (\omega_p^*)^2 \tau_{tr}^*/4\pi \tag{1}$$

in analogy with Drude formula. The effective transport scattering rate $1/\tau_{tr}^*$ characterizes the decay of the current carried by QPs due to collisions involving umklapp effects, and ω_p^* is the low energy effective plasma frequency of QPs and can be expressed in terms of QP velocities and the Landau parameters[5].

The temperature dependence of the transport coefficients beyond the scope of LFL and many salient features seen in correlated oxides, such as their low coherence scale, non saturating resistivities and anomalous transfer of spectral weight, are described well in studies of doped Hubbard model within the framework of dynamical field mean theory (DMFT) (for early reviews of this topic see [6, 7]). A complete understanding of the transport anomalies has been reached recently[8–10]. As in the Prange-Kadanoff theory[4], the QPs are resilient surviving in a broad region above T_{LFL} [9] and a quantum kinetic equation provides a quantitative description of the transport[10] .

While in the electron-phonon coupled system treated in Ref. 4 the Fermi liquid parameters such as the quasiparticle velocities and therefore ω_p^* are temperature independent, they are strongly temperature dependent in the doped Mott insulator within DMFT due to changes in the Fermi surface at high temperatures [8, 9] and a strong temperature dependence of the effective mass at intermediate temperatures [9, 10]. This strong temperature dependence of ω_p^* hides the more conventional temperature dependence of $1/\tau_{tr}^*$ in the resistivity, which is quadratic in a broad region of temperatures and has saturating behavior at high temperatures [10]. Strong temperature dependence in the QP electronic structure with the resulting temperature dependence of ω_p^* and $1/\tau_{tr}^*$ thus provides a simple scenario to describe the anomalous transport of correlated metals.

In this Letter, we provide experimental and theoretical evidences that this picture holds beyond the DMFT treatment of simplified Hubbard Model, and is indeed relevant to real materials. We focus on V_2O_3. This archetypal correlated material provided the first experimental corroboration of the validity of the DMFT picture of Mott transition[11] and is still a subject of intense experimental studies[12–16]. We propose formulas to extract the effective plasma frequency ω_p^* and effective

scattering rate $1/\tau^*_{tr}$ from optical conductivity and show that they display the predicted temperature dependence. We contrast their temperature dependence to that of the plasma frequency and scattering rate extracted from the standard extended Drude analysis.

In correlated systems the optical conductivity is usually parametrized with the so-called extended Drude analysis in terms of two frequency dependent quantities, the scattering rate $1/\tau(\omega)$ and the mass enhancement $m^*(\omega)/m_b$ [17],

$$\sigma(\omega) = \sigma_1(\omega) + i\sigma_2(\omega) = \frac{\omega_p^2}{4\pi}\frac{1}{-i\omega\frac{m^*(\omega)}{m_b} + 1/\tau(\omega)}. \quad (2)$$

The plasma frequency ω_p is obtained with the partial sum rule $\frac{\omega_p^2}{8} = \int_0^\Omega \sigma_1(\omega)d\omega$ and depends on the cutoff Ω chosen so as to exclude interband transitions. To test the theory, instead we focus on quantities that have a simple QP interpretation, namely $1/\tau^*_{tr}$ and $(\omega^*_p)^2$, from low frequency optical conductivity extracted as follows,

$$(\omega^*_p)^2 = 4\pi\frac{\sigma_1^2+\sigma_2^2}{\sigma_2/\omega}|_{\omega\to 0}, \qquad 1/\tau^*_{tr} = \frac{\sigma_1}{\sigma_2/\omega}|_{\omega\to 0}, \quad (3)$$

When a direct determination of the imaginary part of optical conductivity (as for example in ellipsometry measurements) is not available, they can be extracted from $\sigma_1(\omega)$ only, using

$$\frac{\sigma_2(\omega)}{\omega}|_{\omega\to 0} = -\frac{1}{\pi}\int_{-\infty}^{\infty}\frac{1}{\omega'}\frac{\partial\sigma_1(\omega')}{\partial\omega'}d\omega'. \quad (4)$$

Comparing with extended Drude analysis, we have $(\omega^*_p)^2 = \frac{m_b}{m^*(0)}\omega_p^2$, $\frac{1}{\tau^*_{tr}} = \frac{m_b}{m^*(0)}\frac{1}{\tau(0)}$. Thus this analysis is related to extended Drude analysis, but free of partial sum rule. Similar low frequency analysis has been used in previous works[17–21], however the temperature dependence of ω^*_p was not the focus of those studies.

We apply the proposed analysis to V_2O_3, a prototype of metal insulator transition (MIT) [22, 23]. Pure V_2O_3 is a paramagnetic metal (PM) at ambient condition. It enters antiferromagnetic insulating state (AFI) below $T_N \simeq 150$K with a concomitant structural transition, and the AFI can be quenched by Ti-doping or pressure. The PM can be turned into the paramagnetic insulator (PI) by slight Cr-doping, which induces a first order isostructural transition with a small change in c/a ratio, indicating a typical band-controlled MIT scenario[24]. This first order transition ends at a second order critical point at temperature around 400K [12, 23]. The PM phase exhibits significant signatures of correlations, for instance, a pronounced QP peak and a broad lower Hubbard band were revealed in photoemission spectroscopy measurements [25–27]. The PM phase is a Fermi liquid at low temperature when AFI state is suppressed [28].

Fig 1(a)(b) shows the measured optical conductivity $\sigma(\omega) = \sigma_1(\omega) + i\sigma_2(\omega)$ of pure V_2O_3 in PM phase[15].

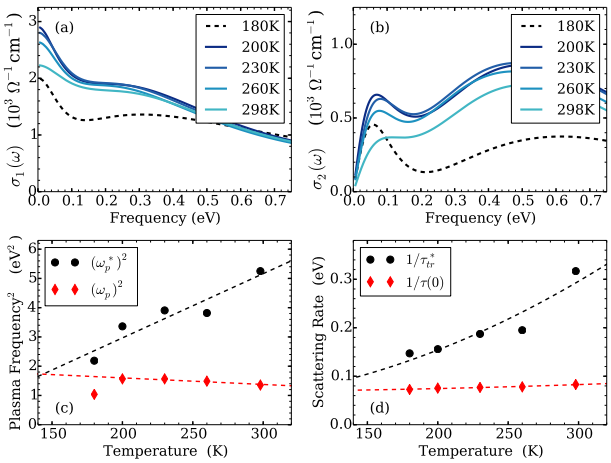

FIG. 1. Optical conductivity (a) $\sigma_1(\omega)$ and (b) $\sigma_2(\omega)$ of V_2O_3 at different temperature is taken from Ref. [15], where dashed lines indicate data at $T = 180$K very close to MIT. (c) $(\omega^*_p)^2$ and (d) $1/\tau^*_{tr}$ of V_2O_3 are extracted according to Eqn. 3. For comparison, ω_p^2 and $1/\tau(0)$ extracted from the extended Drude analysis are also shown. Dashed lines are guides for the eyes by fitting $(\omega^*_p)^2$ (ω_p^2, excluding $T = 180$K) and $1/\tau^*_{tr}$ ($1/\tau(0)$) to linear and parabolic functions respectively.

Pronounced Drude peaks show up even when the resistivity is high (of the order of 1 $m\Omega^{-1}cm^{-1}$) and does not follow T^2-law[12, 29]. The Drude peak diminishes gradually upon increasing temperature, except at the lowest temperature where the transport is probably affected by the precursor of ordered phase. ω^*_p and $1/\tau^*_{tr}$ extracted according to Eqn. 3 are shown in Fig 1(c)(d). We find that $(\omega^*_p)^2$ increases with increasing temperature. This is in contrast with the Drude plasma frequency square $(\omega_p)^2$ obtained by the partial sum rule with a cut off $\Omega = 140$meV, which slightly decreases[15] except at the lowest temperature. $1/\tau^*_{tr}$ increases with increasing temperature and has the same trend as the scattering rate extracted with extended Drude analysis at zero frequency $1/\tau(0)$, but with a much stronger temperature dependence. The experimental data is consistent with an $(\omega^*_p)^2$ which has a term linear and a $1/\tau^*_{tr}$ which is quadratic in temperature, revealing a Fermi liquid behavior that is hidden in $1/\tau^*_{tr}$. The analysis of the experimental data, thus corroborates the main qualitative predictions of the DMFT description of transport properties in simple model Hamiltonian[10].

We now argue that realistic LDA+DMFT [30, 31] calculations describe well the optical properties as well as the extracted quantities ω^*_p and $1/\tau^*_{tr}$, hence a local approximation, which ignores vertex corrections, is sufficiently accurate to capture the experimental trends. LDA+DMFT investigations on V_2O_3 by several groups have successfully described the properties of this material near the MIT [32–36]. The correlation in V_2O_3 is due to the partially filled narrow d-orbitals with a nominal oc-

cupancy $n_d = 2$. The two electrons mainly populate the e_g^π and a_{1g} states of vanadium due to surrounding oxygen octahedron with trigonal distortion.

We perform the LDA+DMFT calculations with an implementation as described in Ref. [37], which is based on WIEN2k package[38]. We use projectors within a large (20eV) energy window constructing local orbitals. This study thus includes explicitly the oxygen orbitals hybridizing with the d orbitals. The interaction is applied to e_g^π and a_{1g} orbitals only. To solve the impurity problem, we use continuous-time quantum Monte-Carlo method with hybridization expansion [39, 40]. The Brillouin zone integration is performed with a regular 12x12x12 mesh. The muffin-tin radius is 1.95 and 1.73 Bohr radius for V and O respectively. The structure is taken from pure V_2O_3 at room temperature and only paramagnetic state is considered.

The Coulomb interaction U and the Hund's coupling J are set to 6.0eV and 0.8eV respectively. They are consistent with the ones used in previous studies [32–36], but U is slightly larger. This is because in previous studies the relevant correlated orbitals are more extended due to downfolding or projection onto a small energy window and hence experience a reduced repulsion. With these parameters the calculated total spectra is consistent with experiment photoemission spectroscopy measurements [25–27]. The occupancies of e_g^π and a_{1g} orbitals at $T = 200K$ are 1.60 and 0.50 respectively, in good agreement with X-ray absorption spectroscopy [41] measurements and previous LDA+DMFT calculations [35]. These parameters place V_2O_3 on the metallic side but close to the MIT in the phase diagram (temperature versus interaction strength) with the temperature at critical endpoint of the first order MIT close to the experimental findings [12, 23].

We calculate the optical conductivity in a broad temperature range as shown in Fig. 2(a). The main feature of the experimental optical conductivity, the Drude peak and the shoulder structure at about 0.1eV as well as their scale , are reasonably reproduced in our calculations. The Drude peak is gradually diminished and merges with the shoulder structure at around 400K, in agreement with experiments [42]. Therefore LDA+DMFT calculation provides a satisfactory description of the optical properties of V_2O_3. From the optical conductivity $(\omega_p^*)^2$ and $1/\tau_{tr}^*$ are extracted using Eqn. 3. As shown in Fig 2(b)(c), they agree reasonably well with those extracted from experimental data. In particular the same trends found with the experimental data, thus the main charactersistics of the "hidden" Fermi liquid behavior, show up more clearly in the broad temperature range studied in our calculations: $(\omega_p^*)^2$ appears linear and a $1/\tau_{tr}^*$ appears quadratic versus temperature. Therefore the proposed analysis of both the experimental data and the first principle calculations reveals significant temperature dependence of QPs in terms of $(\omega_p^*)^2$ and an extended quadratic temperature dependence of $1/\tau_{tr}^*$, but not of $1/\tau(0)$.

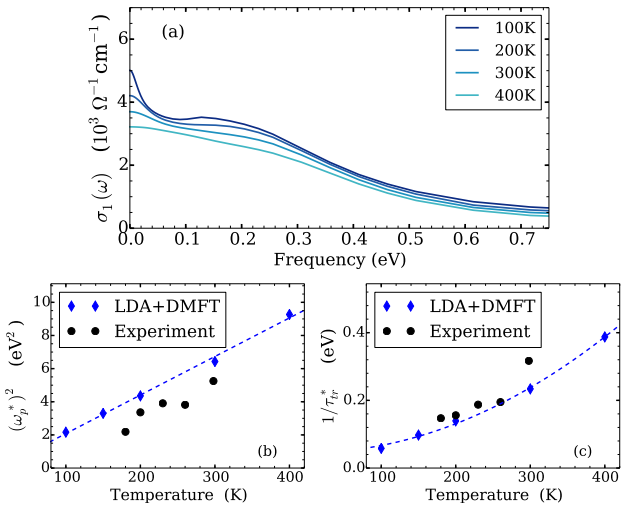

FIG. 2. (a) Optical conductivity of V_2O_3 calculated with LDA+DMFT. The effective plasma frequency (b) and effective scattering rate (c) are extracted using Eqn. 3 and compared to those extracted from experimental data. Dashed lines are guides to the eyes by fitting $(\omega_p^*)^2$ and $1/\tau_{tr}^*$ to linear and parabolic functions respectively.

To further understand the observations, let us recall the QP interpretation of low frequency optical conductivity in the DMFT treatment of the doped single band Hubbard model. In this case, $\sigma(\omega)|_{\omega\to 0} = 2Z_{qp}\Phi^{xx}(\bar{\mu})\frac{1}{-i\omega+2/\tau_{qp}^*}$, in which Z_{qp} and τ_{qp}^* are the QP weight and life time, Φ is the transport function $\Phi^{xx}(\epsilon) = \sum_{\mathbf{k}}(\partial\epsilon_{\mathbf{k}}/\partial\mathbf{k}_x)^2\delta(\epsilon-\epsilon_{\mathbf{k}})$ and $\bar{\mu}$ is the effective chemical potential of QPs[10]. Applying the analysis in Eqn. 3, we have $(\omega_p^*)^2 = 8\pi Z_{qp}\Phi^{xx}(\bar{\mu})$ and $1/\tau_{tr}^* = 2/\tau_{qp}^*$, therefore in this simple model, $(\omega_p^*)^2$ and $1/\tau_{tr}^*$ directly relate to the QP weight and life time. In situations where $\Phi(\bar{\mu})$ varies little with temperature, the observations above imply a strong temperature dependence of Z and $1/\tau_{qp}^*$. We emphasize that although a strong dependence of scattering rate is generally expected in a Fermi liquid, the temperature dependence of QP weight is not, but it was observed in model studies[9, 10].

We then extract from our calculated self energies, the QP weight (which is the inverse of the mass enhancement within single site DMFT) defined as $Z = (1-\frac{\partial Re\Sigma(\omega)}{\partial\omega})^{-1} = m_b/m^*$ and the scattering rate defined as $2/\tau_{qp}^* = -2ZIm\Sigma(0)$. The QP weight and the QP scattering rate are shown in Fig. 3(a)(b). There is orbital differentiation between e_g^π and a_{1g}orbitals as pointed out in earlier LDA+DMFT studies [32, 34]. Both orbital self energies exhibit the same trends observed in the studies of model hamiltonians: Z increases almost linearly with temperature and $1/\tau_{qp}^*$ is nearly quadratic in temperature for each orbital in the temperature range considered. Note that e_g^π orbitals have a much larger spectra weight

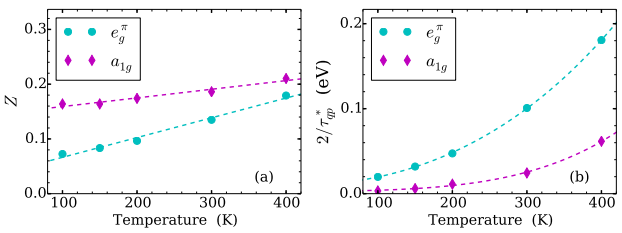

FIG. 3. The temperature dependence of (a) QP weight $Z = (1 - \frac{\partial Re\Sigma(\omega)}{\partial \omega})^{-1}$ and (b) effective scattering rate $2/\tau_{qp}^* = -2ZIm\Sigma(0)$ of V_2O_3 extracted from LDA+DMFT self energies for e_g^π and a_{1g} orbitals. Dashed lines are guides for the eyes by fitting Z and $2/\tau_{qp}^*$ to linear and parabolic functions respectively

at the Fermi level than the a_{1g} orbital thus dominate the transport. This pronounced temperature dependence is consistent with that of $(\omega_p^*)^2$ and $1/\tau_{tr}^*$ extracted from optical conductivity. Therefore the properties of the underlying QPs, especially the temperature dependence of the QP weight and the QP scattering rate, are captured in our analysis on optical conductivities. We note that in addition the temperature dependence of underlying QPs manifest itself in the temperature dependence of the effective chemical potentials of QPs (see online supplementary), which also contribute to the the temperature dependence of $(\omega_p^*)^2$.

We expect that this picture of anomalous transport in correlated materials is not limited to V2O3 and is in fact generally applicable to various strongly correlated metals . To check the validity of this general conjecture we apply the same analysis to experimental data of $NdNiO_3$ (NNO) film on $LaAlO_3$ (LAO) substrate. NNO is another typical correlated material exhibiting temperature-driven MIT[43]. While deposited as film on LAO substrate, the MIT can be quenched so that it remains metallic down to very low temperature [44]. High quality optical conductivities of NNO film are taken from Ref 45 as shown in Fig 4(a)(b). We note that the resistivity is not T^2-like except possibly at the lowest temperature $T = 20K$ [44]. We perform the same analysis as above in V_2O_3. $(\omega_p^*)^2$ and $1/\tau_{tr}^*$ are shown in Fig. 4(c)(d) in comparison with ω_p^2 and $1/\tau(0)$ obtained by extended Drude analysis with a cutoff of $\Omega = 125$meV. Again we have the same features as in V_2O_3: $(\omega_p^*)^2$ is linear in temperature and has the opposite trend with $(\omega_p)^2$, while $1/\tau_{tr}^*$ has a more pronounced quadratic behavior in a wide temperature range well above T_{LFL}.

In conclusion, in this Letter we point out that the anomalous transport properties observed in many transition metal oxides arise from a temperature dependent $(\omega_p^*)^2$ and $1/\tau_{tr}^*$. We establish that by analyzing both the experimental and the theoretical data. This scenario calls for further investigations in other compounds, starting from systems where there are already prelimi-

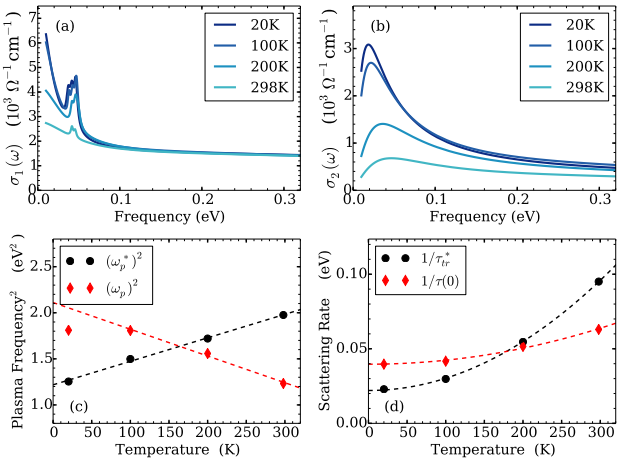

FIG. 4. Optical conductivity (a) $\sigma_1(\omega)$ and (b) $\sigma_2(\omega)$ of NNO film on LAO substrate at different temperature is taken from Ref. [45], from which (c) $(\omega_p^*)^2$ and (d) $1/\tau_{tr}^*$ are extracted according to Eqn. 3. For comparison, ω_p^2 and $1/\tau(0)$ extracted from the extended Drude analysis are shown. Dashed lines are guides for the eyes by fitting $(\omega_p^*)^2$ (ω_p^2 excluding $T = 20$K) and $1/\tau_{tr}^*$ ($1/\tau(0)$) to linear and parabolic functions respectively.

nary indications that it applies, for example, $CaRuO_3$ where a similar low energy analysis was performed [18]. In many other systems, such as nickelate and pnictides, a temperature dependent $m^*(0)/m_b$ is seen in the extended Drude analysis [46, 47]. Thus an extraction of the low energy effective plasma frequency $(\omega_p^*)^2$ as outlined in this paper, and a comparison with $(\omega_p)^2$ from the partial sum rule would be illuminating. Recent optical spectroscopy studies of underdoped cuprates [48] at low temperatures revealed temperature independent $(\omega_p^*)^2$ and a quadratic temperature dependence in $1/\tau_{tr}^*$, consistent with the earlier theoretical predictions of cluster DMFT [49]. It would be interesting to extend the measurements to higher temperatures where deviations from canonical Fermi liquid are expected. Finally high resolution studies using spectroscopies such as ARPES and STM in quasiparticle interference mode would be very useful to separate the various contributions to the temperature dependence of $(\omega_p^*)^2$ by probing directly the electronic structure.

We acknowledge very useful discussions with A. Georges and P. Armitage. This work was supported by NSF DMR-1308141 (X. D. and G.K), NSF DMR 0746395 (K. H.) and DOE-BES (A. S. and D. B.).

temperature dependence of momentum-resolved spectra and quasiparticle bands of V_2O_3

Electronic structure of correlated metal has a significant temperature dependence. This can be seen in the momentum-resolved spectra, defined as

$$A(\mathbf{k},\omega) = -\frac{1}{\pi} Im[\frac{1}{\omega + \mu(T) - H_{\mathbf{k}} - \Sigma_{\mathbf{k}}(\omega,T)} \tag{5}$$

in LDA+DMFT calculations, in which $H = -\nabla^2 + V_{ext} + V_H + V_{xc} - \hat{E}V_{dc}$, $\Sigma_{\mathbf{k}}(\omega,T) = \hat{E}_{\mathbf{k}}\Sigma(\omega,T)$, $\hat{E}$ is the embedding operator and $\Sigma(\omega,T)$ is the impurity self energy in orbital space. As mentioned in the main text, the quasiparticles (QPs) are well defined and meaningful for the transport properties even when the scattering rate in the self energy is large. The QP dispersion $\epsilon^*_{\mathbf{k}}$ is defined as the solution to the following equation:

$$\det(\omega + \mu(T) - H_{\mathbf{k}} - Re[\Sigma_{\mathbf{k}}(\omega,T)]) = 0. \tag{6}$$

The spectra $A(\mathbf{k},\omega)$ and the QP dispersion $\epsilon^*_{\mathbf{k}}$ for two different temperature are depicted in Fig. 5(a)(b). We find that increasing temperature broadens the spectra $A(\mathbf{k},\omega)$ significantly due to the temperature dependence of QP scattering rate. The temperature also modifies the QP dispersion in two aspects: with increasing temperature the QP bands near the Fermi level are less renormalized in accordance with the temperature dependence of QP weight shown in the main text, and the QP bands are shifted accordingly. Both effects affect the transport properties. The shifts of the quasiparticles can be described with the effective chemical potential $\bar{\mu}(T) = \mu - Re\Sigma(0,T)$, which in general has an orbital index due to orbital differentiation. Fig. 5(c) shows the temperature dependence of $\bar{\mu}(T)_{e_g^\pi}$ and $\bar{\mu}(T)_{a_{1g}}$. The shifts of QP bands result in a change of Fermi surface upon increasing temperature. We note that our predicted QP bands with full electron calculations are different from those calculated with a downfolded Hubbard model [34], where the orbital polarization was found to be very large and only a single Fermi surface remains. This is because the crystal field splitting of V_2O_3 is mainly hybridization driven and thus better described with p-d like model rather than the Hubbard model. This prediction is to be verified by further detailed experiments especially with angular-resolved photoemission spectroscopy measurements.

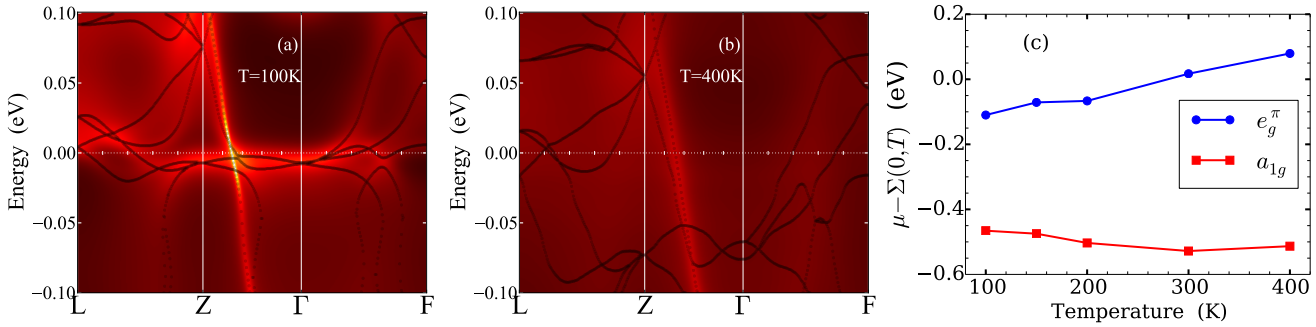

FIG. 5. The calculated momentum-resolved spectra of V_2O_3 at temperature $T = 100$K (a) and $T = 400$K (b). The corresponding QP dispersion $\epsilon^*_{\mathbf{k}}$ computed using Eqn.6 is shown with dots. The effective chemical potentials for e_g^π and a_{1g} orbitals are shown in (c).

[1] V. J. Emery and S. A. Kivelson, Phys. Rev. Lett. **74**, 3253 (1995).
[2] N. Hussey, K. Takenaka, and H. Takagi, Phil. Mag. **84**, 2847 (2004).
[3] O. Gunnarsson, M. Calandra, and J. E. Han, Rev. Mod. Phys. **75**, 1085 (2003).
[4] R. E. Prange and L. P. Kadanoff, Phys. Rev. **134**, A566 (1964).
[5] D. Pines and P. Nozières, *The Theory of Quantum Liquids*.
[6] T. Pruschke, M. Jarrell, and J. Freericks, Advances in Physics **44**, 187 (1995).
[7] A. Georges, G. Kotliar, W. Krauth, and M. J. Rozenberg, Rev. Mod. Phys. **68**, 13 (1996).
[8] G. Pálsson and G. Kotliar, Phys. Rev. Lett. **80**, 4775 (1998).
[9] X. Deng, J. Mravlje, R. Žitko, M. Ferrero, G. Kotliar, and A. Georges, Phys. Rev. Lett. **110**, 086401 (2013).
[10] W. Xu, K. Haule, and G. Kotliar, Phys. Rev. Lett. **111**, 036401 (2013).
[11] M. J. Rozenberg, G. Kotliar, H. Kajueter, G. A. Thomas,

D. H. Rapkine, J. M. Honig, and P. Metcalf, Phys. Rev. Lett. **75**, 105 (1995).
[12] P. Limelette, A. Georges, D. Jrome, P. Wzietek, P. Metcalf, and J. M. Honig, Science **302**, 89 (2003).
[13] S. Lupi, L. Baldassarre, B. Mansart, A. Perucchi, A. Barinov, P. Dudin, E. Papalazarou, F. Rodolakis, J.-P. Rueff, J.-P. Iti, S. Ravy, D. Nicoletti, P. Postorino, P. Hansmann, N. Parragh, A. Toschi, T. Saha-Dasgupta, O. K. Andersen, G. Sangiovanni, K. Held, and M. Marsi, Nature Communications **1**, 105 (2010).
[14] F. Rodolakis, P. Hansmann, J.-P. Rueff, A. Toschi, M. W. Haverkort, G. Sangiovanni, A. Tanaka, T. Saha-Dasgupta, O. K. Andersen, K. Held, M. Sikora, I. Alliot, J.-P. Itié, F. Baudelet, P. Wzietek, P. Metcalf, and M. Marsi, Phys. Rev. Lett. **104**, 047401 (2010).
[15] M. K. Stewart, D. Brownstead, S. Wang, K. G. West, J. G. Ramirez, M. M. Qazilbash, N. B. Perkins, I. K. Schuller, and D. N. Basov, Phys. Rev. B **85**, 205113 (2012).
[16] Y. Ding, C.-C. Chen, Q. Zeng, H.-S. Kim, M. J. Han, M. Balasubramanian, R. Gordon, F. Li, L. Bai, D. Popov, S. M. Heald, T. Gog, H.-k. Mao, and M. van Veenendaal, Phys. Rev. Lett. **112**, 056401 (2014).
[17] D. N. Basov, R. D. Averitt, D. van der Marel, M. Dressel, and K. Haule, Rev. Mod. Phys. **83**, 471 (2011).
[18] S. Kamal, D. M. Kim, C. B. Eom, and J. S. Dodge, Phys. Rev. B **74**, 165115 (2006).
[19] S. J. Youn, T. H. Rho, B. I. Min, and K. S. Kim, physica status solidi (b) **244**, 1354 (2007).
[20] A. Millis, in *Strong interactions in low dimensions*, Physics and Chemistry of Materials with Low-Dimens, Vol. 25, edited by D. Baeriswyl and L. Degiorgi (Springer Netherlands, 2004) pp. 195–235.
[21] N. P. Armitage, (2009), arXiv:0908.1126.
[22] D. B. McWhan, T. M. Rice, and J. P. Remeika, Phys. Rev. Lett. **23**, 1384 (1969).
[23] D. B. McWhan, A. Menth, J. P. Remeika, W. F. Brinkman, and T. M. Rice, Phys. Rev. B **7**, 1920 (1973).
[24] M. Imada, A. Fujimori, and Y. Tokura, Rev. Mod. Phys. **70**, 1039 (1998).
[25] S.-K. Mo, J. D. Denlinger, H.-D. Kim, J.-H. Park, J. W. Allen, A. Sekiyama, A. Yamasaki, K. Kadono, S. Suga, Y. Saitoh, T. Muro, P. Metcalf, G. Keller, K. Held, V. Eyert, V. I. Anisimov, and D. Vollhardt, Phys. Rev. Lett. **90**, 186403 (2003).
[26] F. Rodolakis, B. Mansart, E. Papalazarou, S. Gorovikov, P. Vilmercati, L. Petaccia, A. Goldoni, J. P. Rueff, S. Lupi, P. Metcalf, and M. Marsi, Phys. Rev. Lett. **102**, 066805 (2009).
[27] H. Fujiwara, A. Sekiyama, S.-K. Mo, J. W. Allen, J. Yamaguchi, G. Funabashi, S. Imada, P. Metcalf, A. Higashiya, M. Yabashi, K. Tamasaku, T. Ishikawa, and S. Suga, Phys. Rev. B **84**, 075117 (2011).
[28] D. B. McWhan, J. P. Remeika, J. P. Maita, H. Okinaka, K. Kosuge, and S. Kachi, Phys. Rev. B **7**, 326 (1973).
[29] D. B. McWhan, J. P. Remeika, T. M. Rice, W. F. Brinkman, J. P. Maita, and A. Menth, Phys. Rev. Lett. **27**, 941 (1971).
[30] G. Kotliar, S. Y. Savrasov, K. Haule, V. S. Oudovenko, O. Parcollet, and C. A. Marianetti, Rev. Mod. Phys. **78**, 865 (2006).
[31] K. Held, Advances in Physics **56**, 829 (2007).
[32] K. Held, G. Keller, V. Eyert, D. Vollhardt, and V. I. Anisimov, Phys. Rev. Lett. **86**, 5345 (2001).
[33] M. S. Laad, L. Craco, and E. Müller-Hartmann, Phys. Rev. B **73**, 045109 (2006).
[34] A. I. Poteryaev, J. M. Tomczak, S. Biermann, A. Georges, A. I. Lichtenstein, A. N. Rubtsov, T. Saha-Dasgupta, and O. K. Andersen, Phys. Rev. B **76**, 085127 (2007).
[35] P. Hansmann, A. Toschi, G. Sangiovanni, T. Saha-Dasgupta, S. Lupi, M. Marsi, and K. Held, physica status solidi (b) **250**, 1251 (2013).
[36] D. Grieger, C. Piefke, O. E. Peil, and F. Lechermann, Phys. Rev. B **86**, 155121 (2012).
[37] K. Haule, C.-H. Yee, and K. Kim, Phys. Rev. B **81**, 195107 (2010).
[38] P. Blaha, K. Schwarz, G. K. H. Madsen, D. Kvasnicka, and J. Luitz, *WIEN2K, An Augmented Plane Wave + Local Orbitals Program for Calculating Crystal Properties* (Karlheinz Schwarz, Techn. Universität Wien, Austria, 2001).
[39] K. Haule, Phys. Rev. B **75**, 155113 (2007).
[40] P. Werner, A. Comanac, L. de' Medici, M. Troyer, and A. J. Millis, Phys. Rev. Lett. **97**, 076405 (2006).
[41] J.-H. Park, L. H. Tjeng, A. Tanaka, J. W. Allen, C. T. Chen, P. Metcalf, J. M. Honig, F. M. F. de Groot, and G. A. Sawatzky, Phys. Rev. B **61**, 11506 (2000).
[42] L. Baldassarre, A. Perucchi, D. Nicoletti, A. Toschi, G. Sangiovanni, K. Held, M. Capone, M. Ortolani, L. Malavasi, M. Marsi, P. Metcalf, P. Postorino, and S. Lupi, Phys. Rev. B **77**, 113107 (2008).
[43] J. B. Torrance, P. Lacorre, A. I. Nazzal, E. J. Ansaldo, and C. Niedermayer, Phys. Rev. B **45**, 8209 (1992).
[44] J. Liu, M. Kareev, B. Gray, J. W. Kim, P. Ryan, B. Dabrowski, J. W. Freeland, and J. Chakhalian, Applied Physics Letters **96**, 233110 (2010).
[45] M. K. Stewart, J. Liu, M. Kareev, J. Chakhalian, and D. N. Basov, Phys. Rev. Lett. **107**, 176401 (2011).
[46] M. K. Stewart, C.-H. Yee, J. Liu, M. Kareev, R. K. Smith, B. C. Chapler, M. Varela, P. J. Ryan, K. Haule, J. Chakhalian, and D. N. Basov, Phys. Rev. B **83**, 075125 (2011).
[47] M. M. Qazilbash, J. J. Hamlin, R. E. Baumbach, L. Zhang, D. J. Singh, M. B. Maple, and D. N. Basov, Nat Phys **5**, 647 (2009).
[48] S. I. Mirzaei, D. Stricker, J. N. Hancock, C. Berthod, A. Georges, E. van Heumen, M. K. Chan, X. Zhao, Y. Li, M. Greven, N. Barii, and D. van der Marel, Proceedings of the National Academy of Sciences **110**, 5774 (2013).
[49] K. Haule and G. Kotliar, Phys. Rev. B **76**, 104509 (2007).